

**ANALYSIS OF PROBABILITY OF MISLEADING
INFORMATION FOR LAAS SIGNAL IN SPACE ***

Curtis A. Shively

Center for Advanced Aviation System Development

The MITRE Corporation, McLean VA

ABSTRACT

The Federal Aviation Administration's (FAA's) Local Area Augmentation System (LAAS) provides misleading information when integrity checks at the LAAS ground facility (LGF) and a vertical protection level (VPL) computed in the aircraft allow the navigation system error to exceed acceptable limits without generating an alert. This paper presents a detailed analysis of the probability of misleading information (P_{MI}) in the case of one or two ground reference receiver failures. Performance is computed as a function of the size of the resulting position error. The analysis shows that the aircraft VPL check alone provides a P_{MI} which peaks at the design value and is significant only over a narrow range of position errors. Thus, the aircraft VPL parameters documented in the LAAS Minimum Aviation System

* The contents of this material reflect the views of the author. Neither the Federal Aviation Administration nor the Department of Transportation makes any warranty or guarantee, or promise, expressed or implied concerning the content or accuracy of the views expressed herein.

Performance Standards (MASPS) [1] actually provide significant P_{MI} performance margin.

Consequently, the tolerable a-priori probability of LGF reference receiver failure may be larger than originally assumed.

INTRODUCTION

Background

The LAAS will enhance the performance of GPS so that aircraft can conduct precision approaches to Category I (CAT I) (and eventually to CAT III) weather minimums. Integrity of navigation using LAAS is ensured by checks in the LGF in the range domain, in conjunction with checks in the aircraft in the position domain. The LGF broadcasts differential corrections for each ranging source (satellite or pseudolite) that are the average of corrections from multiple reference receivers. A primary means used by the LGF to ensure integrity of these corrections is known as the Multiple Reference Consistency Check (MRCC). The MRCC function computes a so-called B value, which estimates the error in the correction from a particular reference receiver by comparing it to corrections from the other reference receivers [1]. If a B value exceeds the test threshold, the corresponding correction is excluded from the average. If enough B values fail the test, an entire receiver could be excluded from the averaging process or a ranging source excluded from the broadcast corrections. B values that pass the initial ground screening are then broadcast to the aircraft.

In the aircraft, the B values are combined with the geometry of the particular ranging sources in use to compute protection levels bounding the navigation system error in the position domain. For example, in the vertical dimension, multiple VPLs are computed, each VPL_i corresponding to the hypothesis that the i th individual reference receiver is contributing erroneous measurements to the average corrections from which the aircraft position is derived. Misleading Information (MI) would occur when all VPLs are less than the vertical alert limit (VAL), but the actual navigation system vertical error exceeds VAL [1].

Integrity performance requirements for P_{MI} associated with the LAAS signal in space (SIS) have been established in the LAAS MASPS [1] for two cases: 1) rare-normal (fault-free) operation (denoted H_0) or failure of a single reference receiver (denoted H_1) and 2) all other classes of failures (denoted non- H_0/H_1 failures). The LAAS MASPS also includes an analysis and recommended values for a confidence-interval multiplier K_{MD} to provide the required integrity performance in the VPL test (Table D-8 of [1]).

Given an assumed Gaussian distribution for the confidence interval, the choice of K_{MD} sets the “missed detection” probability that the actual error exceeds the VPL bound. However, it is not clear exactly how this relates directly to P_{MI} , particularly for small errors. Furthermore, the choice of K_{MD} is not related to the performance of integrity monitoring in the LGF. It is merely assumed that the a-priori probability of a failure of a single reference receiver is 10^{-5} , regardless of the size of the error that may be introduced and go undetected. The LAAS MASPS also assumes that neither the VPL check nor ground integrity tests provide any mitigation for non- H_0/H_1 failure cases. This demands that the integrity requirement for non-

H_0/H_1 failure cases be met solely through the a-priori probability of these failures. However, it is conceivable that the integrity checks do possess the ability to detect some types of non- H_0/H_1 failures (e.g., multiple receiver failures), thus potentially allowing a higher probability of such events. Verification of the a-priori probability of single or dual receiver failures to a high level of confidence is difficult. Therefore, it is important to understand whether larger values of these probabilities can be tolerated and the extent to which performance margin is provided by the parameters chosen for the ground and aircraft integrity tests.

Purpose and Organization of Paper

This paper describes an analysis conducted to examine in greater detail the performance of the aircraft VPL check and its relationship to integrity tests done in the LGF. P_{MI} is analyzed for single and dual failures of ground reference receivers as a function of the size of the position error that would result from using the corrections from the failed receiver. The paper begins with a general development of the mathematical expressions for VPL and actual vertical error as a function of the random component that determines P_{MI} . Then, analysis and results are presented first for single failures, followed by the dual failure case. The reader who does not wish to study the mathematical details may choose to focus on the results presented in graphs and the summary at the end of the paper.

VERTICAL PROTECTION LEVEL AND VERTICAL ERROR

This section develops convenient expressions for VPLs and the actual vertical position error. For ease of exposition, the LGF is assumed to include three reference receivers throughout this analysis.

VPLs are computed using B values broadcast by the LGF. Although B values are usually defined in terms of comparisons of differential corrections [1], it is more useful in this analysis to focus only on the errors in the corrections. Thus, the B value for the i th satellite and reference receiver 1, $B_{i,1}$, may be expressed in terms of the error in the differential correction from the j th reference receiver, $e_{i,j}$, as

$$B_{i,1} = \frac{e_{i,1}}{3} - \frac{e_{i,2}}{6} - \frac{e_{i,3}}{6} \quad (1)$$

The corresponding VPL_1 to test the hypothesis that a fault exists in reference receiver 1 may be expressed in terms of the B values for all N satellites in the solution as [1]

$$VPL_1 = \left| \sum_{i=1}^N S_{v,i} B_{i,1} \right| + \frac{K_{MD}}{\sqrt{2}} \sigma_v \quad (2)$$

where $S_{v,i}$ is the vertical coefficient for satellite i in the least squares solution matrix (see 3.1.3.4.5 of [1]),

K_{MD} is the multiplier of σ_v used to set the missed detection probability, and σ_v is the standard deviation of the vertical error given by

$$\sigma_v^2 = \sum_{i=1}^N S_{v,i}^2 \sigma_{\text{gnd_ref}}^2(i) \quad (3)$$

where $\sigma_{\text{gnd_ref}}(i)$ is the standard deviation of the error in the correction for the i th satellite for a single reference receiver. For simplicity, the contributions to σ_v from airborne error and residual tropospheric error are ignored in this analysis.

VPL₁ may also be expressed in terms of the vertical errors E_j corresponding to using the corrections from each reference receiver alone as

$$\text{VPL}_1 = \left| \frac{E_1}{3} - \frac{E_2}{6} - \frac{E_3}{6} \right| + \frac{K_{\text{MD}}}{\sqrt{2}} \sigma_v \quad (4)$$

$$E_j = \sum_{i=1}^N S_{v,i} e_{i,j} \quad (5)$$

Likewise VPL₂ and VPL₃ may be expressed as

$$\text{VPL}_2 = \left| \frac{E_2}{3} - \frac{E_1}{6} - \frac{E_3}{6} \right| + \frac{K_{\text{MD}}}{\sqrt{2}} \sigma_v \quad (6)$$

$$\text{VPL}_3 = \left| \frac{E_3}{3} - \frac{E_1}{6} - \frac{E_2}{6} \right| + \frac{K_{\text{MD}}}{\sqrt{2}} \sigma_v \quad (7)$$

The vertical error E_v resulting from using corrections averaged over the three references is

$$E_v = \frac{E_1}{3} + \frac{E_2}{3} + \frac{E_3}{3} \quad (8)$$

SINGLE FAILURES

VPL and Vertical Error

For the single failure case, it will be assumed that reference 1 is faulty. Thus, this analysis concentrates on VPL_1 because VPL_2 and VPL_3 are designed to detect errors on reference 2 and reference 3, respectively, and have much lower probability of exceeding VAL if VPL_1 does not exceed VAL. It is assumed that $E_1 = E$, a fixed value while E_2 and E_3 are random variables. As of this writing, research is underway to validate the assumption that the error from a fault-free reference receiver can be overbounded by an appropriately chosen Gaussian distribution. Therefore, E_2 and E_3 are assumed to be Gaussian random variables.

For convenience the random variable W is defined representing the scaled sum of E_2 and E_3

$$W = \frac{E_2}{3} + \frac{E_3}{3} \quad (9)$$

characterized by

$$\sigma_W = \frac{\sqrt{2}}{3} \sigma_v \quad (10)$$

Thus, both VPL_1 and the vertical position error E_v can be defined in terms of the fixed parameter E and the Gaussian random component W as

$$VPL_1 = \left| \frac{E}{3} - \frac{W}{2} \right| + \frac{K_{MD}}{\sqrt{2}} \sigma_v \quad (11)$$

$$E_v = \frac{E}{3} + W \quad (12)$$

Constraints on Random Errors for Misleading Information

For misleading information to occur, constraints can be identified on the random component W as a function of the fixed error E . The first constraint is for $|E_v| > VAL$ (the position error is hazardous)

$$|E_v| > VAL \Leftrightarrow \left| \frac{E}{3} + W \right| > VAL \Leftrightarrow W > VAL - \frac{E}{3} \text{ or } W < -VAL - \frac{E}{3} \quad (13)$$

The second constraint is for $VPL_1 < VAL$ (no alert is issued)

$$\begin{aligned}
VPL_1 < VAL &\Leftrightarrow \left| \frac{E}{3} - \frac{W}{2} \right| + \frac{K_{MD}}{\sqrt{2}} \sigma_v < VAL \Leftrightarrow \left| \frac{E}{3} - \frac{W}{2} \right| < TVPL \\
&\Leftrightarrow \frac{2}{3}E - 2VAL + \sqrt{2}K_{MD}\sigma_v < W < \frac{2}{3}E + 2VAL - \sqrt{2}K_{MD}\sigma_v
\end{aligned} \tag{14}$$

$$TVPL = VAL - \frac{K_{MD}}{\sqrt{2}} \sigma_v \tag{15}$$

Conditional Probability of Misleading Information

The conditional probability of MI for a given value of E, $P_{MI|E}$, is found by integrating the probability density function (pdf) of W over the region where both constraints are satisfied

$$P_{MI|E}(E) \cong \int_{LL}^{UL} p(W) dW = \int_{LL}^{UL} \frac{1}{\sqrt{2\pi} \frac{\sqrt{2}}{3} \sigma_v} e^{-\frac{W^2}{2\left(\frac{\sqrt{2}}{3} \sigma_v\right)^2}} dW \tag{16}$$

Since E_v involves the sum of E and W, while VPL_1 involves their difference, it is anticipated that this region will be finite. The lower limit of integration (LL) is given by the larger of the lower limits from the two constraints

$$LL = \max\left(VAL - \frac{E}{3}, \frac{2}{3}E - 2VAL + \sqrt{2}K_{MD}\sigma_v\right) \tag{17}$$

The upper limit of integration (UL) is related only to the VPL₁ constraint

$$UL = \frac{2}{3}E + 2VAL - \sqrt{2}K_{MD}\sigma_v \quad (18)$$

Thus, the maximum value of $P_{MI|E}$ will occur for the value of E where the lower limit of integration is minimized. This occurs at the value of $E = E_{max}$ when the two constraints give the same lower limit.

$$E_{max} = 3VAL - \sqrt{2}K_{MD}\sigma_v \quad (19)$$

The corresponding lower limit is

$$LL(E_{max}) = \frac{\sqrt{2}}{3}K_{MD}\sigma_v = K_{MD}\sigma_w \quad (20)$$

Thus, at $E = E_{max}$, $P_{MI|E}$ takes on the design value that K_{MD} was set to achieve. It is also important to note that while the constraints in general depend on σ_v , $P_{MI|E}(E_{max})$ does not depend on satellite geometry. For any other value of $E \neq E_{max}$, $P_{MI|E}$ will be smaller than its maximum value, because the lower limit of integration will be larger than $K_{MD}\sigma_w$.

Figure 1 presents a graphical illustration of these concepts. This graph plots bounds on W / σ_W for misleading information as a function of E . The bounds are shown for CAT III for particular values of $VAL = 5.3$ m, $K_{FFD} = 5.45$ and $K_{MD} = 4.28$ given in the LAAS MASPS, and the worst allowable geometry ($VDOP = 5.0$, assuming $\sigma_v = VDOP \sigma_{\text{gnd_ref}}$ with $\sigma_{\text{gnd_ref}} = 0.2$ m for Class C receivers) for the predictive VPL equation to be satisfied. Although LAAS will use a weighted position solution, the simplifying assumption that $\sigma_{\text{gnd_ref}}$ does not vary with satellite elevation angle is certainly appropriate for systems using a multipath limiting antenna (highly likely for CAT III). The region between the dashed lines corresponds to no alert ($VPL < VAL$). The region above the upper solid line corresponds to

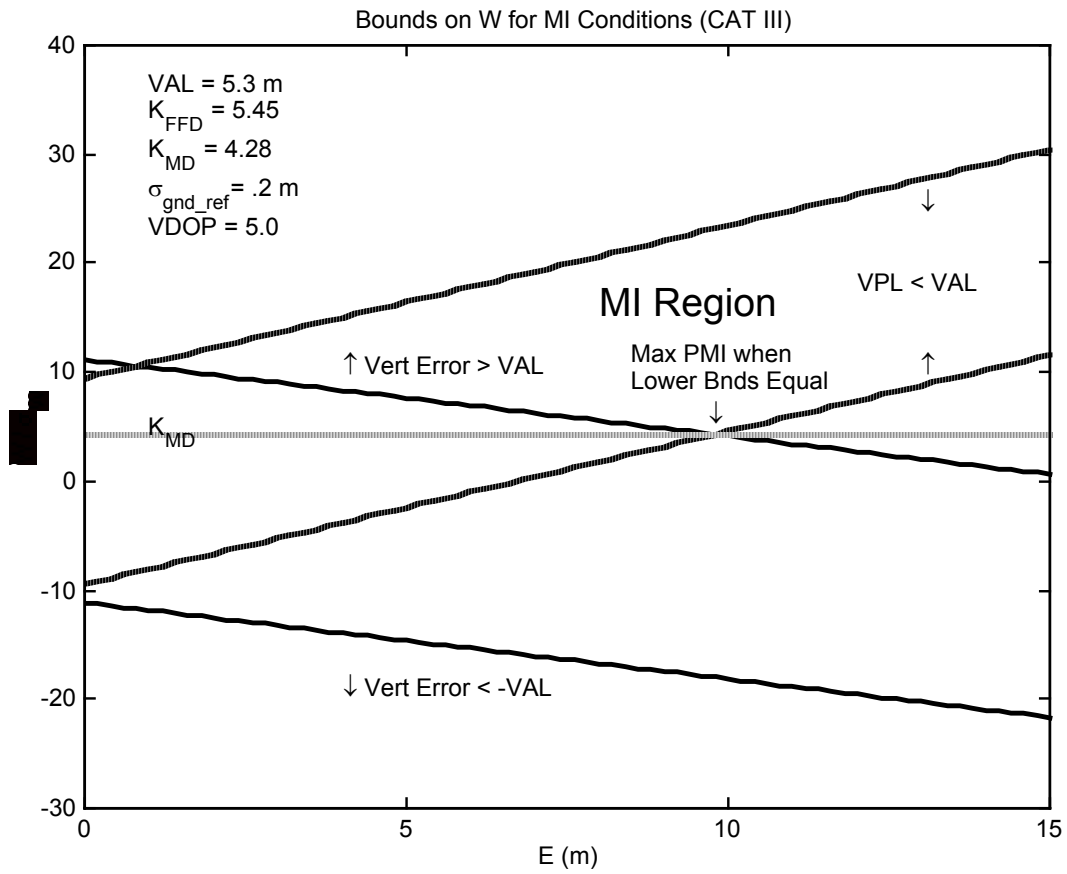


Figure 1: Constraints for Misleading Information at Worst Allowable Geometry (CAT III)

a large vertical error $E_v > VAL$. The MI region is bounded below by the higher of the upper solid line or the lower dashed line. Note that these two lines intersect at $E = E_{max} \sim 9.8$ m and the corresponding lower bound on the random component is $W / \sigma_w = K_{MD}$. A similar graph (not shown) could be plotted for CAT I with $VAL = 10.0$ m, $K_{FFD} = 5.10$ and $K_{MD} = 2.90$, and the corresponding worst allowable geometry ($VDOP = 8.1$, assuming $\sigma_v = VDOP \sigma_{gnd_ref}$ with $\sigma_{gnd_ref} = 0.3$ m for Class B receivers). The resulting $E_{max} \sim 20.0$ m for CAT I.

Plots of $P_{MI|E}$ as a function of $|E|$ are shown in Figure 2 for CAT I and Figure 3 for CAT III, respectively.

Note that in both cases, the peak value of $P_{MI|E}$ and the value of $E = E_{max}$ for which the peak occurs match closely with the values predicted by the above theory. The predicted peak values are $Q(2.90) \sim 1.9 \times 10^{-3}$ for CAT I and $Q(4.28) \sim 1.0 \times 10^{-5}$ for CAT III where $Q(x)$ is defined by the Gaussian distribution

$$Q(x) = \frac{1}{\sqrt{2\pi}} \int_x^{\infty} e^{-\frac{t^2}{2}} dt \quad (21)$$

It should be pointed out that for values of $|E|$ less than E_{max} , the error is likely to go undetected, and P_{MI} is given approximately by $\text{Prob}\{|E_v| > VAL\}$. For $|E|$ greater than E_{max} , the error is likely to exceed

VAL, and P_{MI} is given approximately by $\text{Prob}\{VPL_1 < VAL\}$. Note also that the figures show the total area under the curve, which will be of interest later in the paper for determining the unconditional probability of MI for uniformly distributed E.

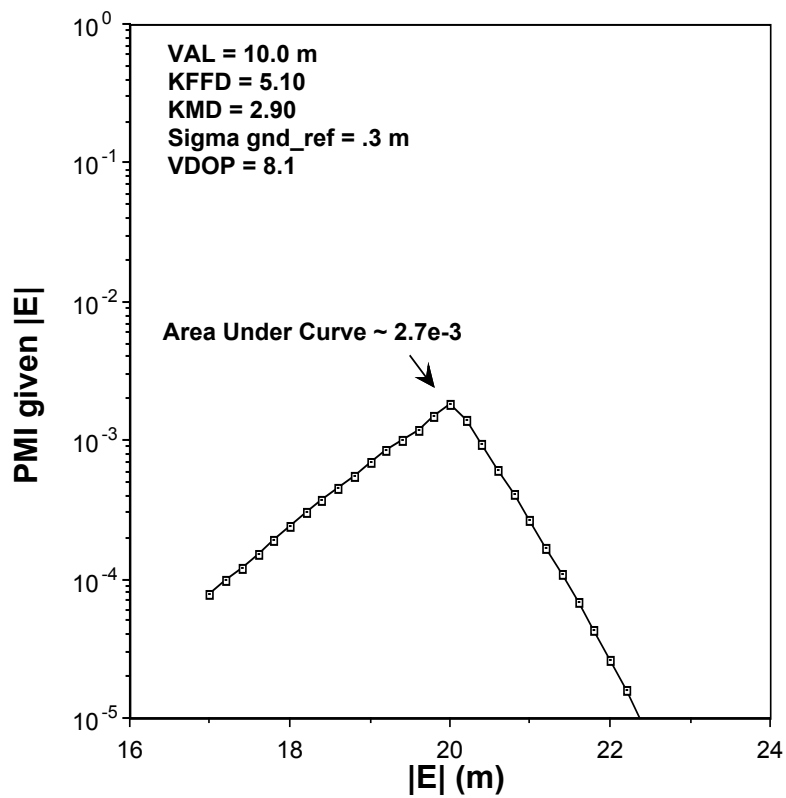
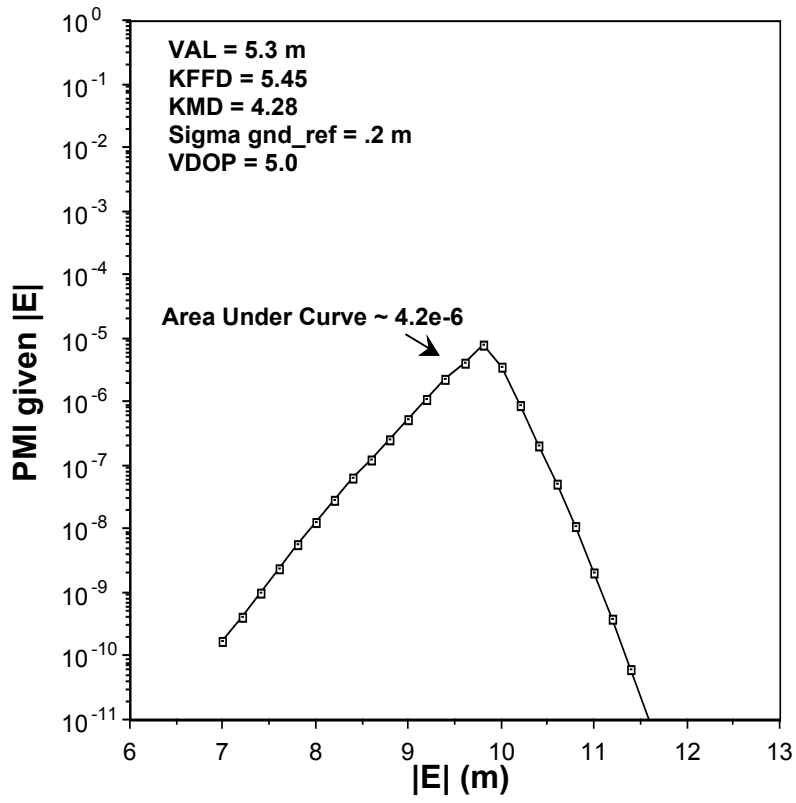


Figure 2: Conditional Probability of Misleading Information (VPL Alone) for Worst Allowable Geometry (CAT I)



**Figure 3: Conditional Probability of Misleading Information
 (VPL Alone) for Worst Allowable Geometry (CAT III)**

Unconditional Probability of Misleading Information

The unconditional probability of misleading information P_{MI} is found by integrating the product of $P_{MI|E}(E)$ and $p(E)$ over all possible values of E

$$P_{MI} = 2 \int_0^{\infty} P_{MI|E}(E) p(E) dE \quad (22)$$

$$p(E) = P_{\text{fault}} \times p_{E|\text{fault}}(E) \quad (23)$$

where P_{fault} is the a-priori probability of a single receiver failure and $p_{E|\text{fault}}$ is the pdf of E given the receiver failure. However, $P_{MI|E}$ is significant for only a small range of E , with a peak at $E = E_{\text{max}}$.

Obviously, if upon failure of the single reference $|E| = E_{\text{max}}$ were always the case, then P_{MI} would be no smaller than the product of P_{fault} and the value for which K_{MD} was set. For the CAT I example given above

$$P_{MI} = Q(2.90) \times P_{\text{fault}} \cong 1.9 \times 10^{-3} \times P_{\text{fault}} \quad (24)$$

Or correspondingly, to achieve the required $P_{MI\text{req}}$, the maximum allowed P_{fault} would be

$$P_{\text{fault max}} = \frac{P_{\text{MIreq}}}{1.9 \times 10^{-3}} = 530 \times P_{\text{MIreq}} \quad (25)$$

However, a more reasonable assumption is that E is uniformly distributed over some interval $\pm L$ m.

Then $p(E) = P_{\text{fault}} / 2L$, $-L \leq E \leq L$. In that case, the maximum value of P_{MI} (the integral in equation (22)) occurs when L is just large enough to include all values of E for which $P_{\text{MI}|E}$ is significant. This condition is met for CAT I if $L = 25$ m (refer to Figure 2). Thus

$$P_{\text{MI}} = \frac{P_{\text{fault}}}{50} 2 \int_0^{25} P_{\text{MI}|E}(E) \cong \frac{2 \times 2.7 \times 10^{-3}}{50} P_{\text{fault}} = 1.08 \times 10^{-4} P_{\text{fault}} \quad (26)$$

$$P_{\text{fault max}} = 9.3 \times 10^3 \times P_{\text{MIreq}} \quad (27)$$

allowing $P_{\text{fault max}}$ to be 18 times larger than if equation (25) must be satisfied. For example if $P_{\text{MIreq}} = 2.5 \times 10^{-8}$ [1], then

$$P_{\text{fault max}} = 2.3 \times 10^{-4} \quad (28)$$

For CAT III the original assumption would require

$$P_{\text{fault max}} = \frac{P_{\text{MIreq}}}{Q(4.28)} = \frac{P_{\text{MIreq}}}{10^{-5}} = 10^5 \times P_{\text{MIreq}} \quad (29)$$

However, as for CAT I, recognizing the extent of E for which $P_{MI|E}$ is significant (refer to Figure 3) and assuming E uniformly distributed ± 15 m gives

$$P_{\text{fault max}} = \frac{30}{2 \times 4.2 \times 10^{-6}} P_{\text{MIreq}} \cong 3.6 \times 10^6 \times P_{\text{MIreq}} \quad (30)$$

allowing a value of P_{fault} which is ~ 36 times larger than needed to satisfy equation (29). For example if

$$P_{\text{MIreq}} \sim 10^{-10} [1]$$

$$P_{\text{fault max}} = 3.6 \times 10^{-4} \quad (31)$$

rather than the value of 10^{-5} needed under the original assumption.

Ground Monitoring - Non MRCC

Recall from the introduction that MRCC applies a threshold to the same B values used in the VPL calculation. Therefore, ground MRCC and the aircraft VPL check are not statistically independent. Consequently, other ground integrity checks that do not compare references will be considered first. One such ground integrity function is known as measurement quality monitoring (MQM) [2.]. Suppose that MQM can effectively bound the error in the correction for reference 1 and the i th satellite, i.e., $|e_{i,1}| \leq$

L_{MQM} . This correction error bound may be transformed into a corresponding position error bound

$L_{MQM}V_{MAX}$ as follows

$$|e_{i,1}| \leq L_{MQM} \Leftrightarrow |E| = \left| \sum_{i=1}^N e_{i,1} S_{v,i} \right| \leq \sum_{i=1}^N |e_{i,1}| |S_{v,i}| \leq L_{MQM} \sum_{i=1}^N |S_{v,i}| = L_{MQM} V_{MAX} \quad (32)$$

$$V_{MAX} = \sum_{i=1}^N |S_{v,i}| ; [3] \quad (33)$$

If it may be assumed that E is essentially uniformly distributed $[-L, L]$ ($L = L_{MQM}V_{MAX}$), then

$$P_{MI} = 2 \int_0^{\infty} P_{MI|E}(E) p(E) dE = 2 \int_0^L P_{MI|E}(E) \frac{P_{fault}}{2L} dE = \frac{P_{fault}}{L} \int_0^L P_{MI|E}(E) dE \quad (34)$$

and additional benefit from MQM is provided only if L is less than E_{max} , the value of E at which $P_{MI|E}$

has a peak. It has been previously shown [3] that

$$\sqrt{2}VDOP \leq V_{MAX} \leq \sqrt{N}VDOP \quad (35)$$

or assuming $N = 9$ satellites in the position solution

$$\sqrt{2}VDOP \leq V_{MAX} \leq 3VDOP \quad (36)$$

Therefore, for CAT I, with a peak in $P_{MI|E}$ at $E_{\max} \sim 20.0$ m and a worst allowable VDOP of 8.1, L_{MQM} must be somewhere in the range

$$0.82 \text{ m} \leq L_{MQM} \leq 1.75 \text{ m} \quad (37)$$

for added benefit from MQM. For CAT III, with a peak in $P_{MI|E}$ at 9.8 m and a worst VDOP of 5.0, L_{MQM} must be somewhere in the range

$$0.65 \text{ m} \leq L_{MQM} \leq 1.39 \text{ m} \quad (38)$$

for added benefit from MQM. It should be noted that since E_{\max} increases with decreasing VDOP (refer to equation (19)), values of L_{MQM} larger than in equations (37) and (38) may still provide some benefit at geometries better than the worst allowed.

Position Domain Monitoring in Aircraft (Illustration Only)

To facilitate developing a relationship between MRCC and P_{MI} , consider first the situation where in addition to the VPL check the aircraft performs a test similar in concept to MRCC (refer back to the introduction), but in the position domain, rather than in the range domain. Such a test would compare

estimates of position error, PD_i , to a threshold T_{PD} . Then for detecting a fault of reference 1, the test would be

$$|PD_1| = \left| \frac{P_1}{3} - \frac{P_2}{6} - \frac{P_3}{6} \right| < T_{PD} \quad (39)$$

$$T_{PD} = K_{FFD} \sigma_{PD} = \frac{K_{FFD} \sigma_v}{\sqrt{6}} \quad (40)$$

or in terms of errors

$$\left| \frac{E}{3} - \frac{E_2}{6} - \frac{E_3}{6} \right| < \frac{K_{FFD} \sigma_v}{\sqrt{6}} \quad \text{or} \quad \left| \frac{E}{3} - \frac{W}{2} \right| < \frac{K_{FFD} \sigma_v}{\sqrt{6}} \quad (41)$$

This test would not generate an alert if

$$\frac{2}{3}E - \frac{2K_{FFD}\sigma_v}{\sqrt{6}} < W < \frac{2}{3}E + \frac{2K_{FFD}\sigma_v}{\sqrt{6}} \quad (42)$$

The lower limit for integration to determine $P_{MI|E}$ from equation (16) then becomes the maximum of three constraints on W , two from equation (17) and the one from equation (42) above

$$LL = \max \left(VAL - \frac{E}{3}, \frac{2}{3}E - 2VAL + \sqrt{2}K_{MD}\sigma_v, \frac{2}{3}E - \frac{2K_{FFD}\sigma_v}{\sqrt{6}} \right) \quad (43)$$

It can be shown that at the worst allowable geometry

$$\frac{K_{FFD}\sigma_v}{\sqrt{6}} = VAL - \frac{K_{MD}\sigma_v}{\sqrt{2}} \text{ or } T_{PD} = T_{VPL} \quad (44)$$

the effective thresholds of the VPL check and the position comparison are identical. Thus, the constraints from VPL₁ (equation (14)) and the position check (equation (42)) are identical, and the position check does nothing to decrease P_{MI}. However, for geometries better than the worst allowed,

$$\frac{K_{FFD}\sigma_v}{\sqrt{6}} < VAL - \frac{K_{MD}\sigma_v}{\sqrt{2}} \text{ or } T_{PD} < T_{VPL} \quad (45)$$

i.e., the position check is a more stringent test. Thus, the peak value of P_{MI}(E) occurs when

$$VAL - \frac{E}{3} = \frac{2}{3}E - \frac{2K_{FFD}\sigma_v}{\sqrt{6}} \quad (46)$$

or at

$$E_{\max} = VAL + \frac{2K_{FFD}\sigma_v}{\sqrt{6}} \quad (47)$$

P_{MI}(E_{max}) is smaller than for VPL alone because the lower limit of integration LL is increased

$$LL = \frac{2}{3} \left(VAL - \frac{K_{FFD}\sigma_v}{\sqrt{6}} \right) > \frac{\sqrt{2}K_{MD}\sigma_v}{3} \quad (48)$$

A graphical illustration of these concepts is presented in Figure 4. This figure is similar to Figure 1, except that a third set of boundaries has been added. The dash-dot lines correspond to constraints on W for no alert based on the position comparison. For the worst allowable geometry (VDOP = 5.0 in this example), these boundaries would coincide with those for the VPL test (dashed lines). However, Figure 4 illustrates the bounds for VDOP = 2.5. In that case, the bounds for $|PD_1| < T_{PD}$ are noticeably tighter.

Note that the lower dot-dashed line intersects the constraint for $E_v > VAL$ at a value higher than $W / \sigma_w = K_{MD}$. Thus, the lower limit of integration for P_{MI} is greater than $K_{MD}\sigma_w$, and the peak value of P_{MI} is smaller than the value that K_{MD} was intended to provide.

Ground Monitoring - MRCC

Now consider the similarity of ground MRCC and the position comparison in the aircraft just analyzed.

MRCC applies a threshold, T_{MRCC} , to each B value (equation (1))

$$\left| \frac{e_{i1}}{3} - \frac{w_i}{2} \right| \leq T_{MRCC} \quad (49)$$

$$w_i = \frac{e_{i,2}}{3} + \frac{e_{i,3}}{3} \quad (50)$$

$$T_{MRCC} = \frac{K_{FFD_gnd}\sigma_{gnd_ref}}{\sqrt{6}} \quad (51)$$

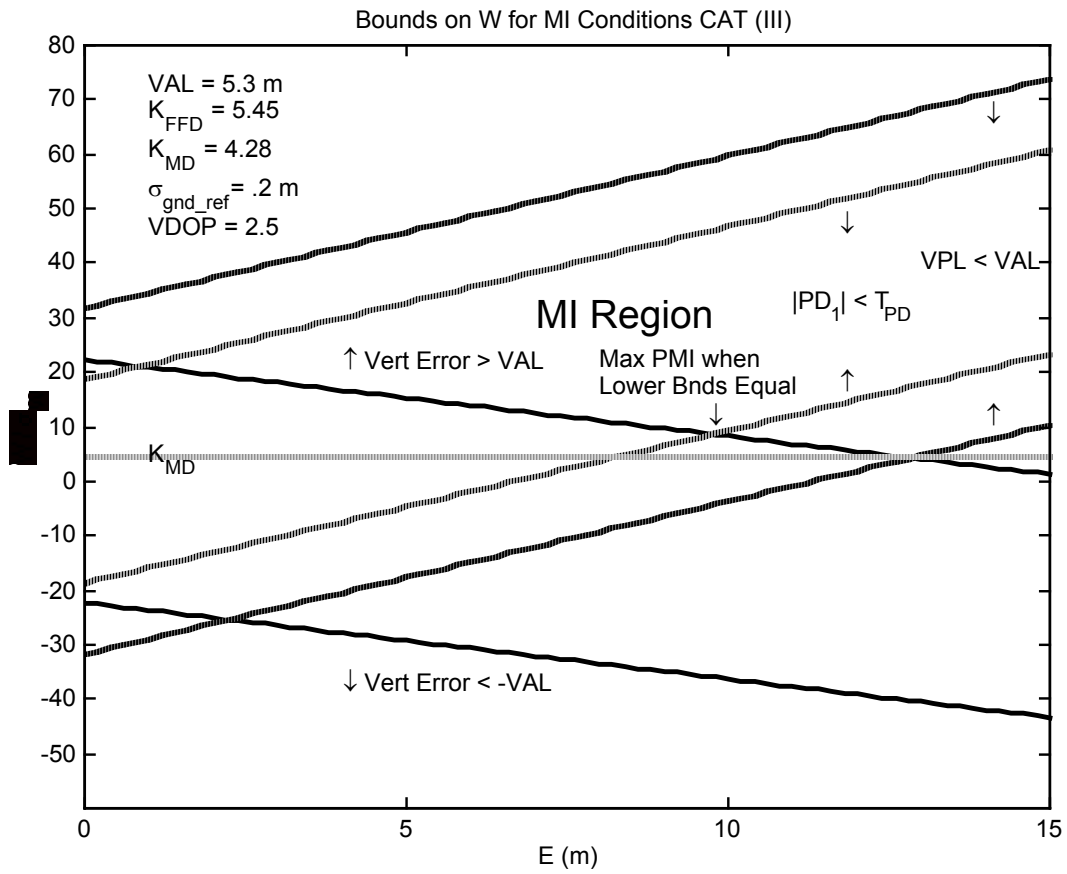


**Figure 4. Constraints for Misleading Information for a Geometry
Twice as Good as the Worst Allowed (CAT III)**

The position error E_1 from using reference 1 corrections is a linear combination of N individual satellite correction errors $e_{i,1}$ from reference 1.

$$E = E_1 = \sum_{i=1}^N S_{v,i} e_{i,1} \quad (52)$$

$$W = \sum_{i=1}^N S_{v,i} w_i \quad (53)$$

For ground monitoring to miss detecting the error E , all N individual satellite tests for reference 1 (equation (49) for $i = 1$ to N) must be less than the MRCC threshold.

This condition establishes a constraint between $e_{i,1}$ and the random error component w_i from the other references. The combination of all these constraints may be translated into a corresponding constraint in the position domain involving $V_{MAX} \sigma_{gnd_ref}$.

$$\sum_{i=1}^N \left| \frac{e_{i,1}}{3} - \frac{w_i}{2} \right| |S_{v,i}| \leq \frac{K_{FFD_gnd} \sigma_{gnd_ref}}{\sqrt{6}} \sum_{i=1}^N S_{v,i} = \frac{K_{FFD_gnd} \sigma_{gnd_ref}}{\sqrt{6}} V_{MAX} \quad (54)$$

$$\left| \frac{E}{3} - \frac{W}{2} \right| = \left| \sum_{i=1}^N \left(\frac{e_{i,1}}{3} - \frac{w_i}{2} \right) S_{v,i} \right| \leq \sum_{i=1}^N \left| \frac{e_{i,1}}{3} - \frac{w_i}{2} \right| |S_{v,i}| \quad (55)$$

$$\left| \frac{E}{3} - \frac{W}{2} \right| \leq \frac{K_{FFD_gnd} \sigma_{gnd_ref}}{\sqrt{6}} V_{MAX} = T_{MRCC} V_{MAX} \quad (56)$$

This test would not generate an alert if

$$\frac{2}{3}E - \frac{2K_{\text{FFD_gnd}}\sigma_{\text{gnd_ref}}}{\sqrt{6}}V_{\text{MAX}} < W < \frac{2}{3}E + \frac{2K_{\text{FFD_gnd}}\sigma_{\text{gnd_ref}}}{\sqrt{6}}V_{\text{MAX}} \quad (57)$$

This condition is similar to that for the position comparison (equation (42)), which would include a factor $\text{VDOP } \sigma_{\text{gnd_ref}}$ if the simplifying assumption is made that an unweighted solution is used. Thus,

$$\sigma_v = \text{VDOP}\sigma_{\text{gnd_ref}} \quad (58)$$

Since $\text{VDOP } \sigma_{\text{gnd_ref}} < V_{\text{MAX}} \sigma_{\text{gnd_ref}}$, MRCC is a less stringent test, and the lower bound on W for misleading information (equation (57)) is lower than for the position comparison (equation (43)).

Therefore, MRCC has a higher peak P_{MI} than does the position comparison (for the same geometry).

Integrity Thresholds and Bounds as Functions of Satellite Geometry

It is informative to compare the integrity thresholds and bounds as a function of satellite geometry. For convenience, recall the following from previous equations

$$T_{\text{VPL}} = \text{VAL} - \frac{K_{\text{MD}}\sigma_v}{\sqrt{2}} = \text{VAL} - \frac{K_{\text{MD}}\text{VDOP}\sigma_{\text{gnd_ref}}}{\sqrt{2}} ; \text{ Aircraft VPL threshold} \quad (59)$$

$$T_{\text{PD}} = \frac{K_{\text{FFD}}\sigma_v}{\sqrt{6}} = \frac{K_{\text{FFD}}\text{VDOP}\sigma_{\text{gnd_ref}}}{\sqrt{6}} ; \text{ Aircraft position domain error threshold} \quad (60)$$

$$T_{\text{MRCC}}V_{\text{MAX}} = \frac{K_{\text{FFD_gnd}}V_{\text{MAX}}\sigma_{\text{gnd_ref}}}{\sqrt{6}} ; \text{ Error bound provided by ground MRCC} \quad (61)$$

$$\sqrt{2}VDOP \leq VMAX \leq \sqrt{N}VDOP \tag{62}$$

These quantities as a function of VDOP are shown in Figure 5 for CAT I and in Figure 6 for CAT III.

Note first that the VPL threshold decreases with degrading geometry (increasing VDOP) while the other three thresholds or bounds all increase as the geometry degrades. This happens because the VPL test is designed to maintain constant integrity, while the other tests and bounds maintain constant fault-free alert

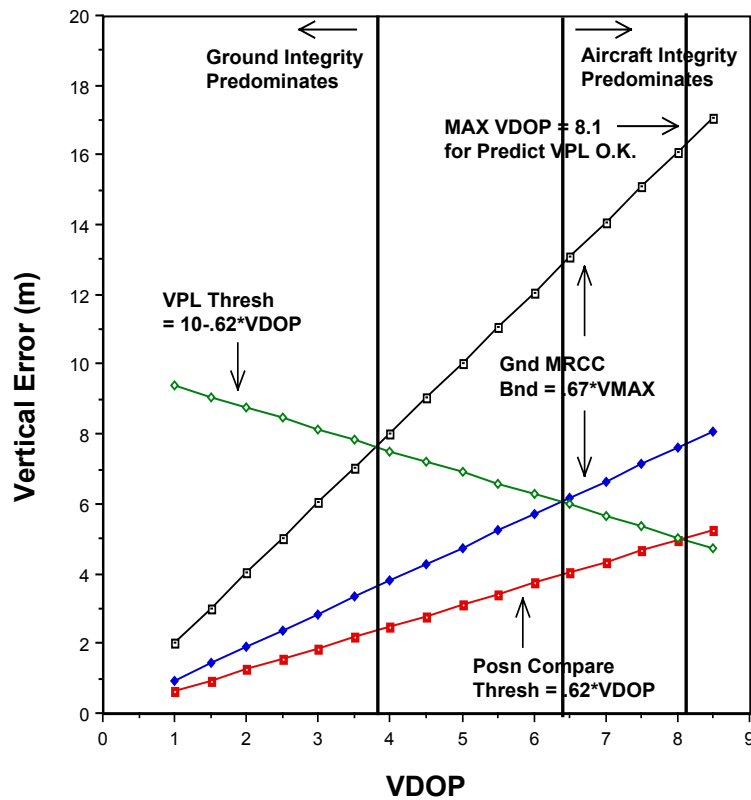


Figure 5. Comparison of Aircraft Integrity Thresholds

and Ground MRCC Error Bound (CAT I)

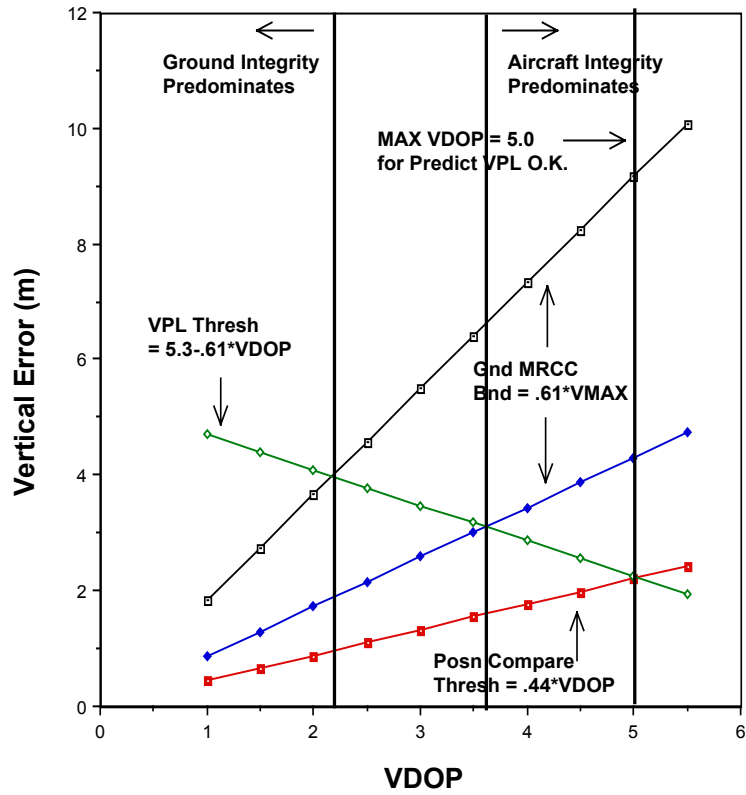


Figure 6. Comparison of Aircraft Integrity Thresholds and Ground MRCC Error Bound (CAT III)

rate. For example, the VPL test subtracts from VAL an integrity margin for the fault-free error from the other reference receivers not being checked. Since this integrity margin increases with degrading geometry, the effective VPL threshold decreases. On the other hand, the hypothetical position comparison uses a threshold T_{PD} which is directly proportional to σ_v , which of course increases along with VDOP. Note that the VPL and position comparison thresholds become equal at the maximum VDOP allowed by predictive VPL (8.1 for CAT I and 5.0 for CAT III). Furthermore, the ground MRCC test uses a range-domain threshold T_{MRCC} which is not a function of geometry at all. T_{MRCC} is based on K_{FFD_gnd} to achieve an acceptable probability of wrong exclusion P_{WE} in MRCC [4]. For CAT I $K_{FFD_gnd} = 5.5$ for $P_{WE} \sim 10^{-3}$, giving $T_{MRCC} = 0.67$ m. For CAT III $K_{FFD_gnd} = 7.5$ for $P_{WE} \sim 10^{-5}$, giving $T_{MRCC} = 0.61$ m. However, the corresponding vertical error is bounded by $V_{MAX} T_{MRCC}$, which does increase in proportion to VDOP.

Since the effective VPL threshold and the ground error limits vary in opposite fashion with VDOP, there is a geometry region where ground integrity predominates over airborne integrity, and vice versa. For example, for smaller VDOPs, ground integrity predominates because the position error limit provided by ground MRCC is lower than the effective threshold of the airborne VPL test. In the figures, this region is delimited by the point where the most conservative bound on V_{MAX} (given by \sqrt{N} VDOP, assuming $N = 9$) intersects the VPL threshold line. This dividing line occurs at about VDOP = 3.8 for CAT I and at about VDOP = 2.2 for CAT III. For VDOPs smaller than these values, the VPL bound can never exceed VAL, given the size of the threshold T_{MRCC} used to limit the B values broadcast by the ground system.

A second region is identified for large VDOPs delimited by the point where the least conservative bound on VMAX (given by $\sqrt{2}$ VDOP) intersects the VPL threshold line. This dividing line occurs at about VDOP = 6.4 for CAT I and VDOP = 3.6 for CAT III. For VDOPs larger than this, it is possible that B values not rejected by the ground MRCC test could produce a VPL exceeding VAL, and the airborne test would predominate in this case. In the geometry region between these two VDOP limits, the integrity check that predominates will depend on the exact value of VMAX for each particular geometry.

Maximum Conditional $P_{MI|E}$ as a Function of Satellite Geometry

A corresponding observation to that just made for the integrity thresholds and bounds can be made for peak $P_{MI|E}$. The variation of peak $P_{MI|E}$ with satellite geometry is shown in Figure 7 for CAT I and in Figure 8 for CAT III. The curves plot $P_{MI|E}(E_{max})$ versus VDOP up to the maximum allowed by predictive VPL (8.1 for CAT I and 5.0 for CAT III). Note that in both figures the curve for the VPL test alone is flat since $P_{MI|E}(E_{max})$ is always equal to the value for which K_{MD} was designed, independent of geometry. Note further that (as discussed above) $P_{MI|E}(E_{max})$ for the position comparison also matches the K_{MD} design value at the worst allowed VDOP, but decreases rapidly as VDOP improves. As discussed above, this happens because the position check provides a lower threshold than the VPL check. Note also that $P_{MI|E}(E_{max})$ for VPL and MRCC follow the K_{MD} design value for some VDOPs smaller than the maximum VDOP. However, even though $VMAX > VDOP$, this curve does begin to fall off rapidly for VDOP less than the value where the MRCC bound is smaller than the effective VPL threshold

(refer to the previous discussion). Two cases are plotted corresponding to the limits of the relationship between VMAX and VDOP ($V_{MAX} = \sqrt{2} \text{ VDOP}$ and $V_{MAX} = \sqrt{N} \text{ VDOP}$, assuming $N = 9$).

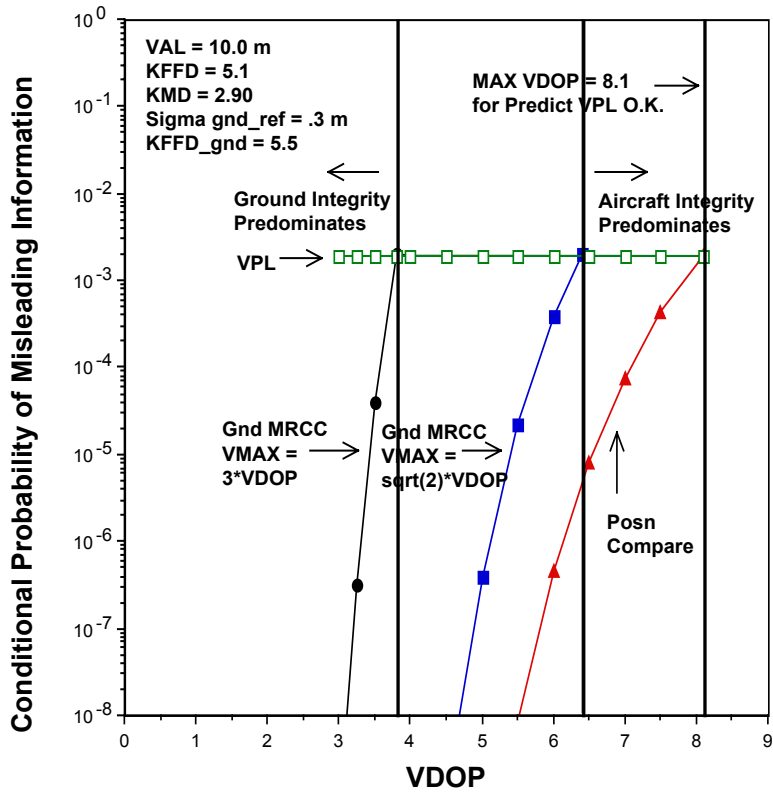


Figure 7. Maximum Conditional Probability of Misleading Information versus VDOP (CAT I)

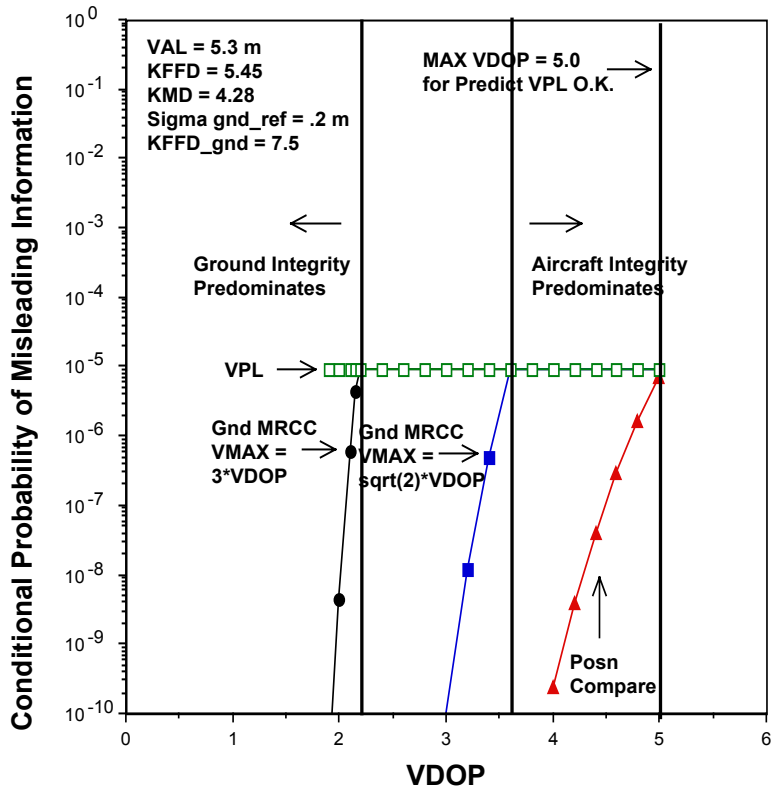


Figure 8. Maximum Conditional Probability of Misleading Information versus VDOP (CAT III)

DUAL FAILURES

For the dual failure case, assume that both references 1 and 2 are faulty, producing vertical errors E_1 and E_2 (not necessarily equal), and E_3 is Gaussian distributed with zero mean and standard deviation equal to σ_v .

Constraints on Random Error for Misleading Information

The following are constraints on E_3 for $|E_v| > VAL$ (error is hazardous) and all $VPL_i < VAL$ (no alert)

$$|E_v| > VAL \Leftrightarrow \left| \frac{E_1}{3} + \frac{E_2}{3} + \frac{E_3}{3} \right| > VAL \Leftrightarrow E_3 > 3VAL - E_1 - E_2 \text{ or } E_3 < -3VAL - E_1 - E_2 \quad (63)$$

$$|VPL_1| < VAL \Leftrightarrow -6T_{VPL} + 2E_1 - E_2 < E_3 < 6T_{VPL} + 2E_1 - E_2 \quad (64)$$

$$|VPL_2| < VAL \Leftrightarrow -6T_{VPL} + 2E_2 - E_1 < E_3 < 6T_{VPL} + 2E_2 - E_1 \quad (65)$$

$$|VPL_3| < VAL \Leftrightarrow -3T_{VPL} + \frac{E_1}{2} + \frac{E_2}{2} < E_3 < 3T_{VPL} + \frac{E_1}{2} + \frac{E_2}{2} \quad (66)$$

$$T_{VPL} = VAL - \frac{K_{MD}}{\sqrt{2}} \sigma_v \quad (67)$$

Conditional Probability of Misleading Information Given E_1 and E_2

The conditional probability of misleading information given E_1 and E_2 , denoted $P_{MI|E_1,E_2}(E_1,E_2)$, is found by integrating the Gaussian pdf of E_3 over the region where the above constraints are satisfied.

$$P_{MI|E_1,E_2}(E_1, E_2) \cong \int_{LL}^{UL} p(E_3) dE_3 = \int_{LL}^{UL} \frac{1}{\sqrt{2\pi\sigma_v}} e^{-\frac{E_3^2}{2\sigma_v^2}} dE_3 \quad (68)$$

$$LL = \max \left[3VAL - E_1 - E_2, -6T_{VPL} + 2E_1 - E_2, -6T_{VPL} + 2E_2 - E_1, -3T_{VPL} + \frac{E_1}{2} + \frac{E_2}{2} \right] \quad (69)$$

$$UL = \min \left[6T_{VPL} + 2E_1 - E_2, 6T_{VPL} + 2E_2 - E_1, 3T_{VPL} + \frac{E_1}{2} + \frac{E_2}{2} \right] \quad (70)$$

Since it is readily observed that the result is negligible unless E_1 and E_2 have the same sign and

$$P_{MI|E_1,E_2}(-E_1, -E_2) = P_{MI|E_1,E_2}(E_1, E_2) \quad (71)$$

attention is focused on the region where $E_1 > 0$ and $E_2 > 0$.

Plots of equal value contours of $P_{MI|E_1,E_2}(E_1,E_2)$ for $E_1 > 0$ and $E_2 > 0$ are shown in Figure 9 for CAT I and Figure 10 for CAT III. Note that the contours are symmetric about the line $E_1 = E_2$ and are centered

at the point $E_1 = E_2 = 15.1$ m for CAT I and $E_1 = E_2 = 7.6$ m for CAT III. Note also that

$P_{M|E_1, E_2}(E_1, E_2)$ decreases rapidly for values of E_1 and E_2 not within a few meters of the central point.

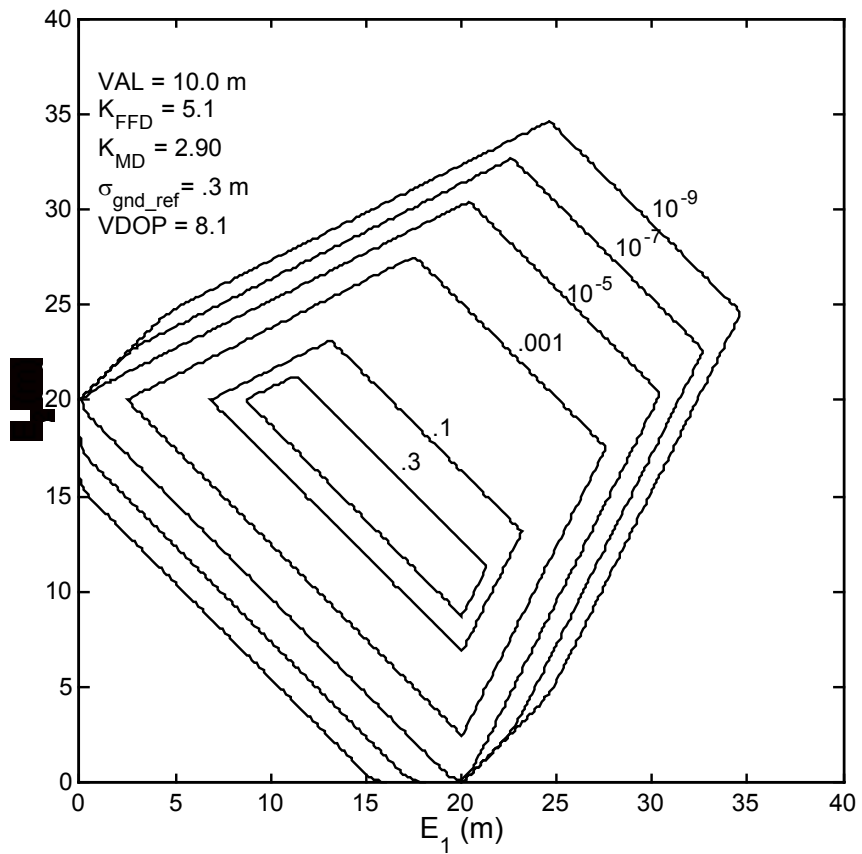


Figure 9. Conditional Probability of Misleading Information

Given E_1, E_2 for Worst Allowable Geometry (CAT I)

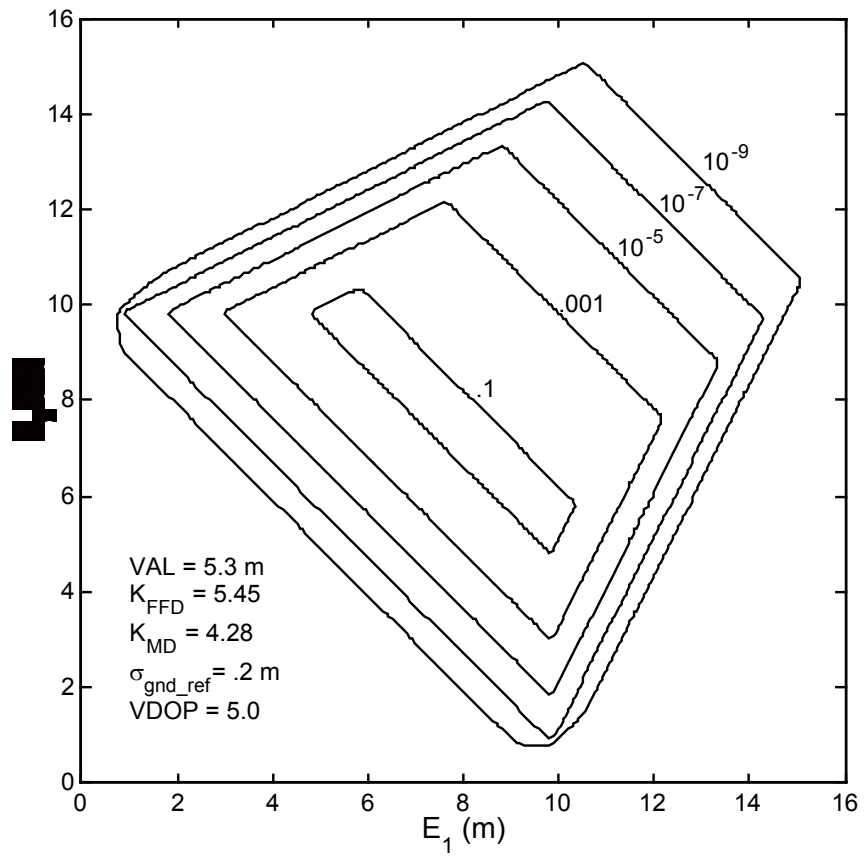


Figure 10. Conditional Probability of Misleading Information

Given E_1, E_2 for Worst Allowable Geometry (CAT III)

Probability of Misleading Information Assuming E_1 and E_2 are Uniformly Distributed

Suppose the position errors E_1 and E_2 due to faults on references 1 and 2 are independent and uniformly distributed over $[-U,U]$. The resulting probability of misleading information (denoted $P_{\text{MI}|\text{faults}}$) is then

$$P_{\text{MI}|\text{faults}} = 2 \int_0^U \int_0^U \frac{1}{4U^2} P_{\text{MI}|E_1, E_2}(E_1, E_2) dE_1 dE_2 = \int_0^U \int_0^U \frac{2}{4U^2} \int_{LL}^{UL} \frac{1}{\sqrt{2\pi}\sigma_v} e^{-\frac{E_3^2}{2\sigma_v^2}} dE_3 dE_1 dE_2 \quad (72)$$

with the limits of integration LL and UL for the Gaussian pdf of E_3 given in equations (69) and (70).

Plots of $P_{\text{MI}|\text{faults}}$ as a function of the maximum error U are given in Figure 11 for CAT I and Figure 12 for CAT III. An understanding of these graphs is facilitated by referring back to the contour plots of $P_{\text{MI}|E_1, E_2}(E_1, E_2)$ in Figures 9 and 10, and thinking of integrating over the region $0 \leq E_1 \leq U$, $0 \leq E_2 \leq U$.

Consider the CAT I case. For small maximum errors U (say < 10 m), no significant values of $P_{\text{MI}|E_1, E_2}(E_1, E_2)$ are included. As U increases, more significant values of $P_{\text{MI}|E_1, E_2}(E_1, E_2)$ are included in the integration. However, when the maximum error increases beyond ~ 20 to 25 m, $P_{\text{MI}|E_1, E_2}(E_1, E_2)$ is no longer significant, and the integral would remain constant except for the factor of $1/U^2$ in the joint pdf of E_1 and E_2 . Therefore, $P_{\text{MI}|\text{faults}}(U)$ reaches a peak value (0.033) near $U \sim 23$ m. If E_1 and E_2 are

uniformly distributed over a lesser or greater extent, $P_{MI|faults}$ is somewhat smaller. In the CAT III case,

$P_{MI|faults}(U)$ reaches a peak value of 0.0089 near $U \sim 10$ m.

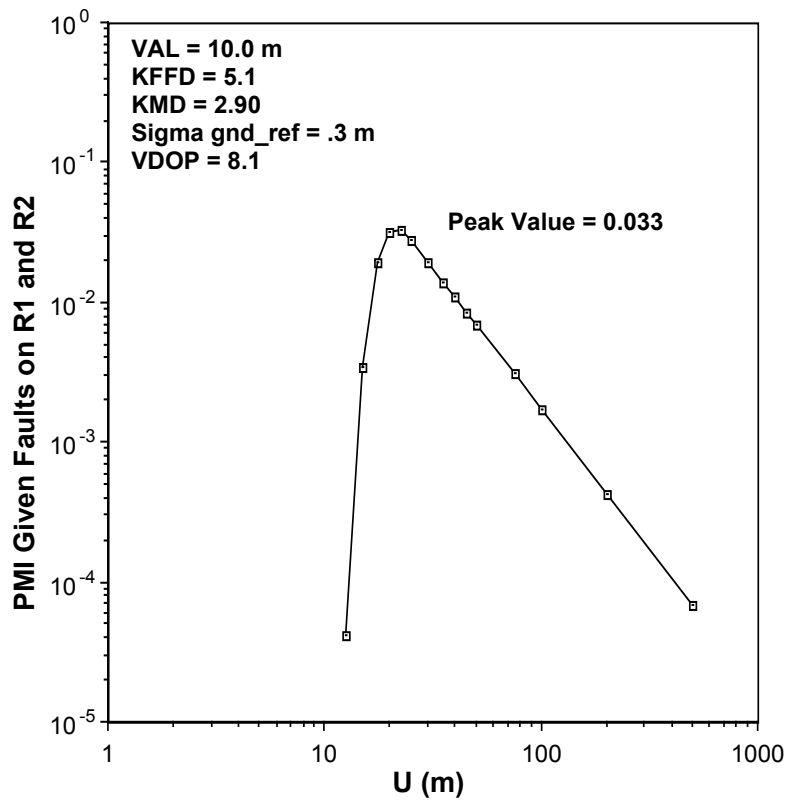


Figure 11. Probability of Misleading Information Assuming E_1 and E_2 are Uniformly Distributed $[-U,U]$ (CAT I)

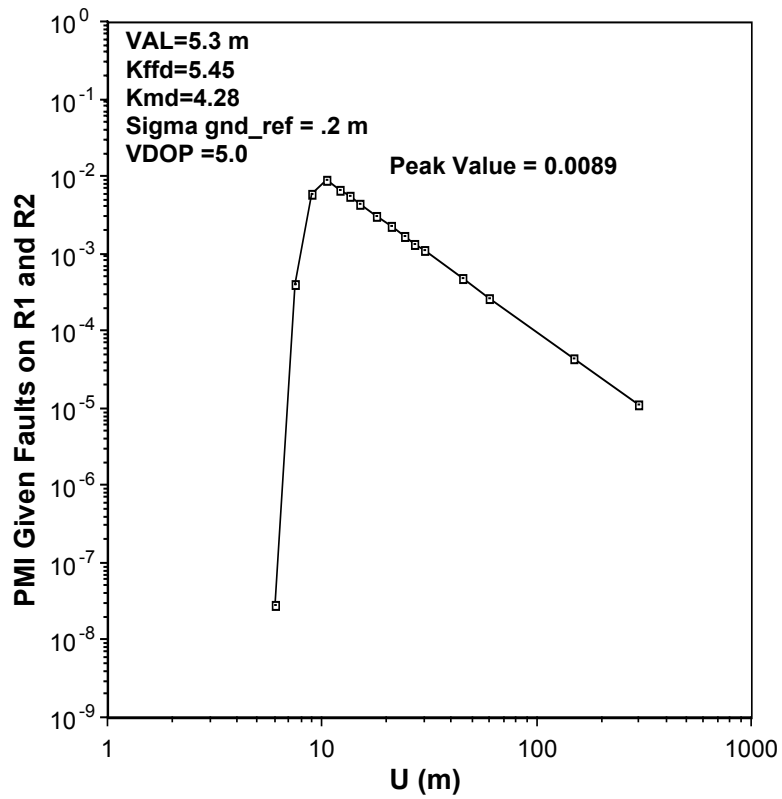


Figure 12. Probability of Misleading Information Assuming
 E_1 and E_2 are Uniformly Distributed $[-U,U]$ (CAT III)

It is desirable to determine the tolerable a-priori probability of dual faults (denoted P_{faults}) that will allow the P_{MI} integrity requirement to be met. Suppose that the two faults are independent and $P_{\text{faults}} = (P_{\text{fault}})^2$ where P_{fault} is the a-priori probability of a single reference receiver fault. Therefore

$$P_{\text{MI}} = P_{\text{faults}} P_{\text{MI}|\text{faults}} = P_{\text{fault}}^2 P_{\text{MI}|\text{faults}} \quad (73)$$

or given the required P_{MI} the corresponding P_{faultmax} is given by

$$P_{\text{fault max}} = \sqrt{\frac{P_{\text{MIreq}}}{P_{\text{MI}|\text{faults}}}} \quad (74)$$

For CAT I $P_{\text{MIreq}} = 1.5 \times 10^{-7}$ and for CAT III $P_{\text{MIreq}} = 7.5 \times 10^{-10}$ (assuming the total integrity risk allocated to non- H_0/H_1 failures is associated with dual receiver failures) [1]. Prior to this analysis, it was pessimistically assumed that $P_{\text{MI}|\text{faults}} = 1$. In that case, the maximum allowed P_{fault} would be $P_{\text{faultmax}} = \sqrt{P_{\text{MIreq}}} = 3.9 \times 10^{-4}$ for CAT I and 2.7×10^{-5} for CAT III. However, it was just shown that for uniformly distributed E_1 and E_2 , the peak value for CAT I is $P_{\text{MI}|\text{faults}} = 0.033$ and for CAT III is $P_{\text{MI}|\text{faults}} = 0.0089$. Therefore, for CAT I, P_{faultmax} can be $1/\sqrt{0.033} \sim 5.5$ times larger, or 2.1×10^{-3} , and for CAT III, P_{faultmax} can be $1/\sqrt{0.0089} \sim 10.6$ times larger, or 2.9×10^{-4} .

It should be pointed out that the above observations might be too optimistic. The occurrence of dual faults may not be independent events and the resulting errors may not be uncorrelated, as assumed in the analysis. Therefore, further investigation is needed to determine the extent to which P_{faultmax} can be increased in practice.

SUMMARY

An analysis was performed of the conditional probability of misleading information ($P_{\text{MI}|E}$) as a function of the vertical error E due to fault of a single LAAS ground reference receiver. $P_{\text{MI}|E}$ was found to have a peak value equal to the design value set by the K_{MD} parameter in the aircraft VPL equation and to be significantly lower for values of E smaller or larger than the value where the peak occurs (E_{max}).

Consequently, the unconditional P_{MI} provided by the VPL test is better than expected (even at the worst allowable geometry). Therefore, if the original requirement for a-priori probability of ground receiver fault is met, overall integrity performance margin is provided. On the other hand, verification testing of ground receivers might be relaxed somewhat, because a larger value of the true a-priori probability of fault could be tolerated.

A hypothetical position comparison in the aircraft (which fixes the probability of fault-free detection rather than the probability of missed detection as does the VPL test) provides a peak $P_{\text{MI}|E}$ equal to that

from the VPL test at the worst allowable geometry and significantly smaller at better geometries. Ground monitoring involving quantities other than the B values used in the VPL computation can provide further benefit if the error can be bounded at a value less than E_{\max} . Ground monitoring which does compare the B values (such as MRCC) predominates over the aircraft VPL check at good geometries and reduces the peak P_{MI} to a level that is significantly below the design value.

An analysis was also performed for $P_{MI|E_1,E_2}$ as a function of the size of errors E_1 and E_2 due to simultaneous faults of two ground reference receivers. Although the VPL check is not intended to mitigate dual failures, $P_{MI|E_1,E_2}$ was found to have a peak value somewhat less than unity and to be significant only for a narrow range of values of E_1 and E_2 . Consequently, a larger than previously assumed a-priori probability of dual ground receiver faults could potentially be tolerated, depending on the extent to which the faults or resulting errors are actually independent, as was assumed in the analysis. Furthermore, additional improvement in $P_{MI|E_1,E_2}$ can be achieved if ground monitoring which does not use B values can effectively bound E_1 and E_2 below the value where the peak $P_{MI|E_1,E_2}$ occurs.

ACKNOWLEDGMENTS

The author wishes to thank Ray Swider and Karl Kaser of the FAA LAAS Program for sponsoring this work. Special thanks to Dan O’Laughlin and Ron Braff of MITRE/CAASD for reviewing the draft and

providing helpful comments. The author is also grateful to the Institute of Navigation's independent reviewer for performing a thorough and insightful evaluation of the paper.

REFERENCES

1. RTCA SC-159 WG-4A, *Minimum Aviation System Performance Standards for the Local Area Augmentation System (LAAS)*, Draft 006, March 4, 1998.
2. LAAS Key Technical Advisors, *FAA LAAS Ground System Functions*, Draft 2.1, June 18, 1998.
3. Fernow J.P., and R. Loh, *Description of Integrity Concepts for a GPS Wide-Area Augmentation System (WAAS)*, Proceedings of the 1994 National Technical Meeting of The Institute of Navigation, San Diego, CA, January 24-26, 1994, pp. 127-135.
4. Shively, C., *Performance Analysis of Alternative Methods for LAAS Multiple Reference Consistency Check*, Proceedings of the 54th Annual Meeting of The Institute of Navigation, Denver, CO, June 1-3, 1998, pp. 187-198.

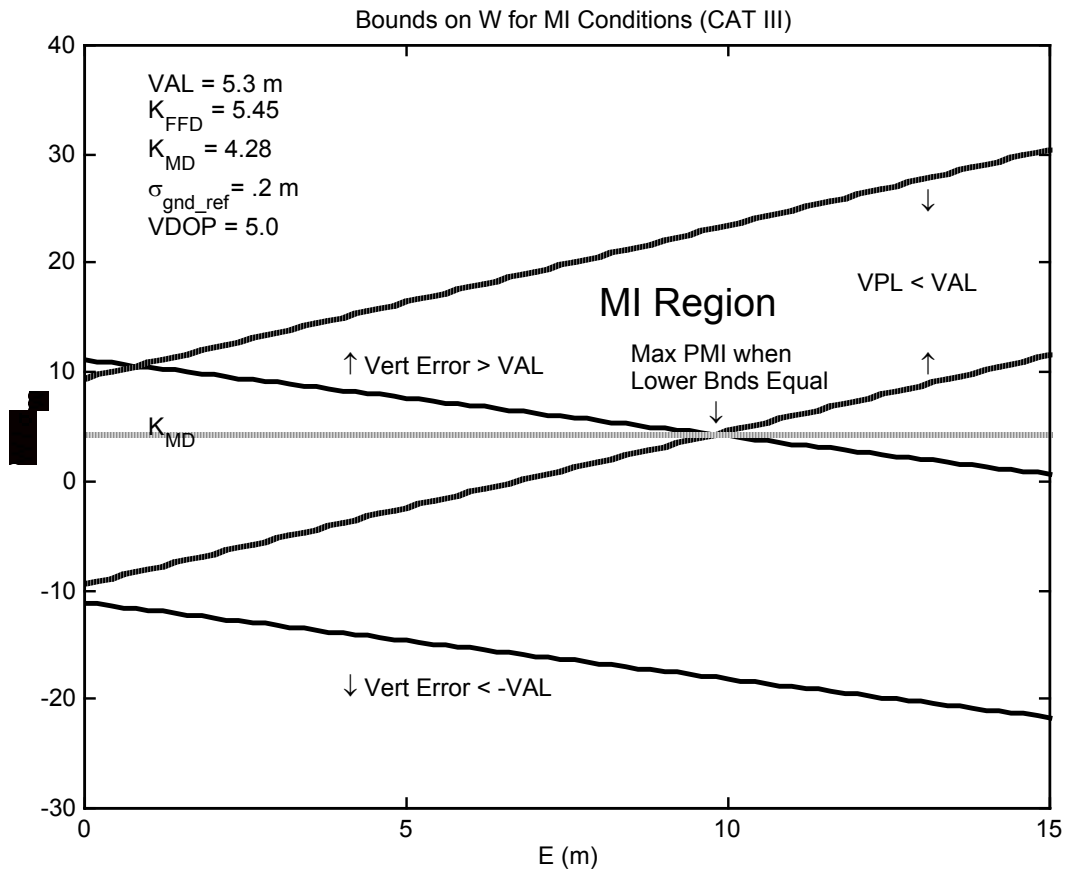
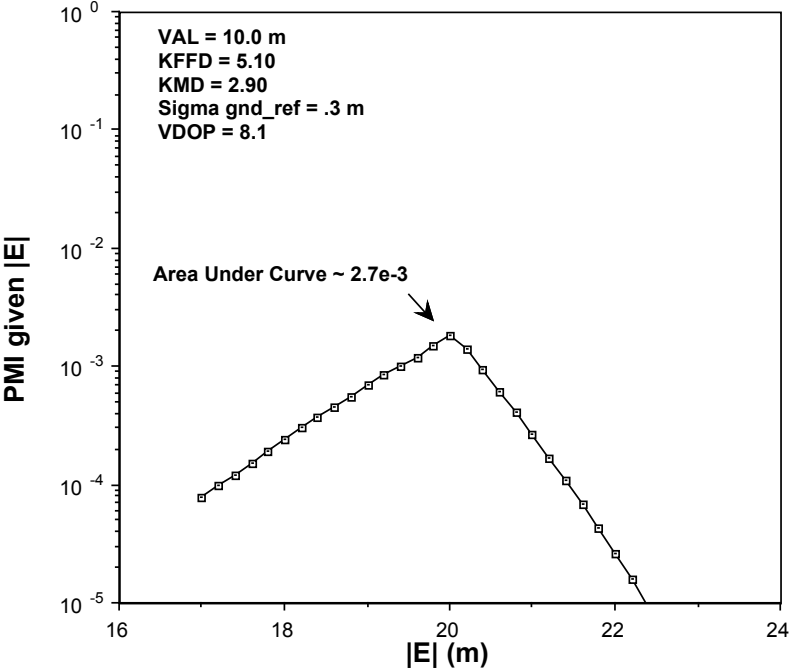
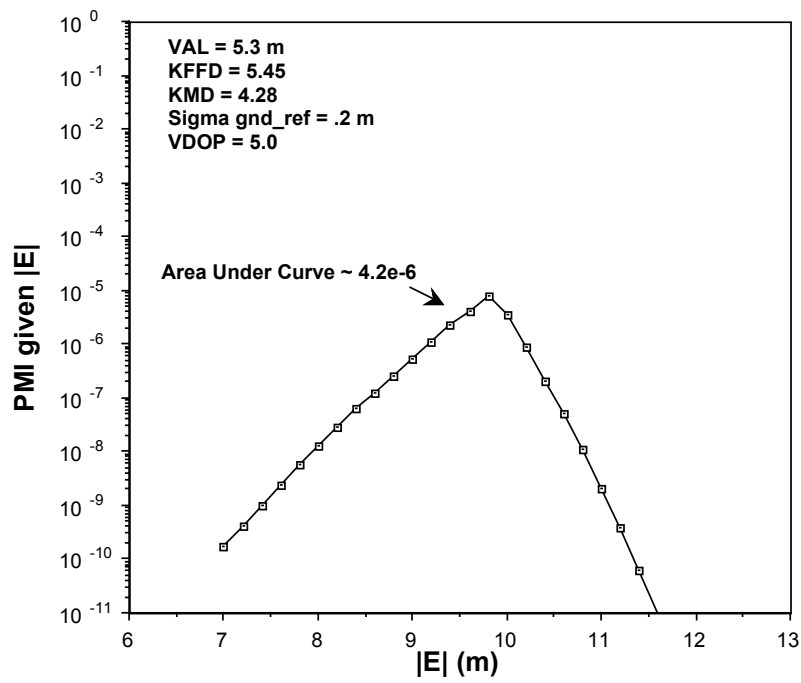


Figure 1: Constraints for Misleading Information at Worst Allowable Geometry (CAT III)



**Figure 2: Conditional Probability of Misleading Information
(VPL Alone) for Worst Allowable Geometry (CAT I)**



**Figure 3: Conditional Probability of Misleading Information
(VPL Alone) for Worst Allowable Geometry (CAT III)**

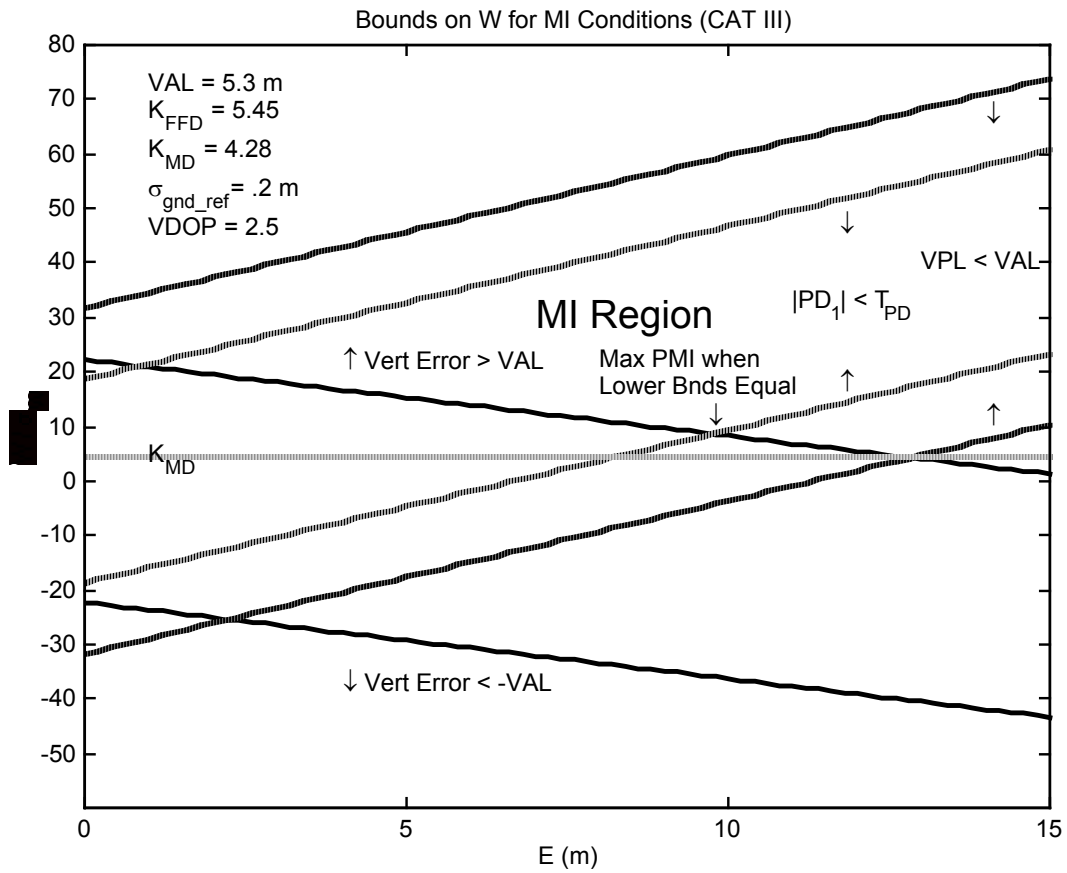


**Figure 4. Constraints for Misleading Information for a Geometry
Twice as Good as the Worst Allowed (CAT III)**

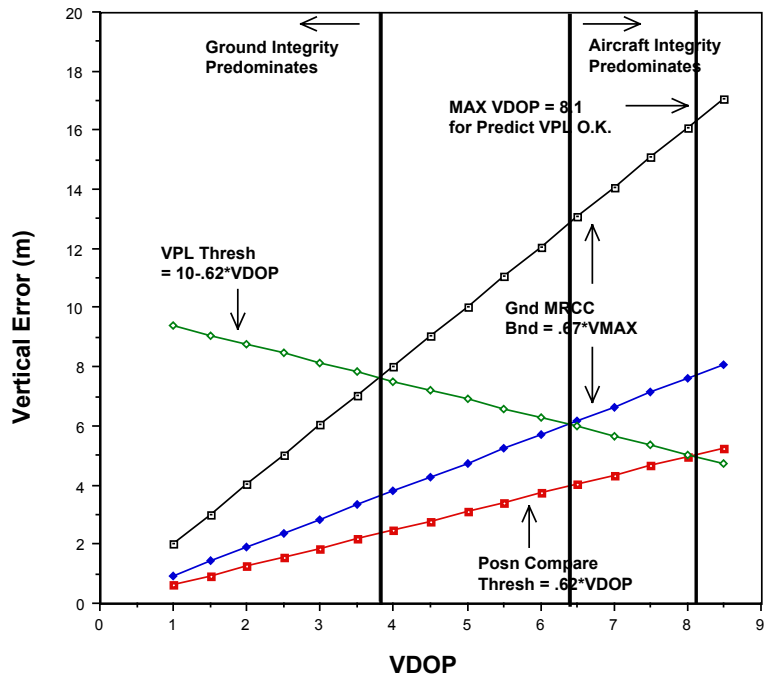


**Figure 5. Comparison of Aircraft Integrity Thresholds
and Ground MRCC Error Bound (CAT I)**

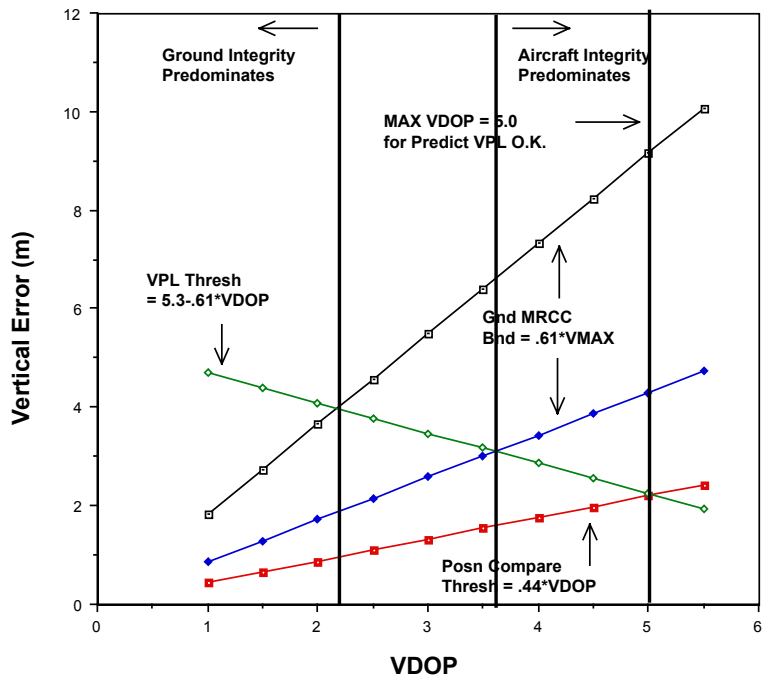


Figure 6. Comparison of Aircraft Integrity Thresholds
and Ground MRCC Error Bound (CAT III)

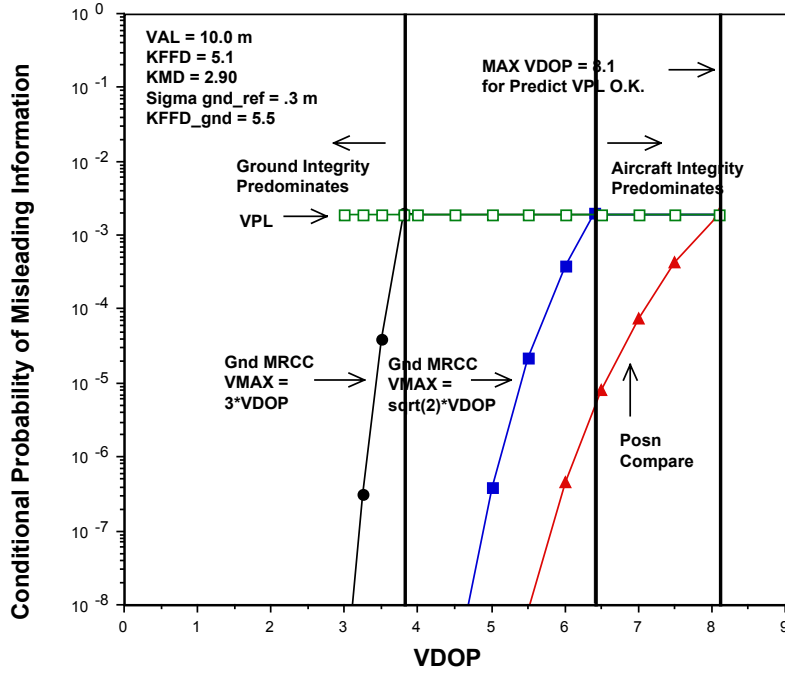


Figure 7. Maximum Conditional Probability of Misleading Information versus VDOP (CAT I)

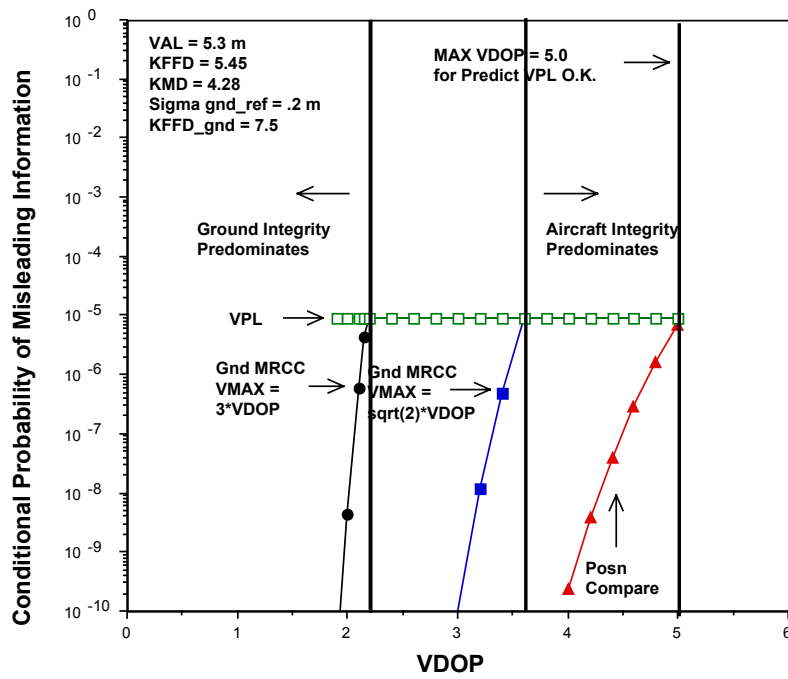


Figure 8. Maximum Conditional Probability of Misleading Information versus VDOP (CAT III)

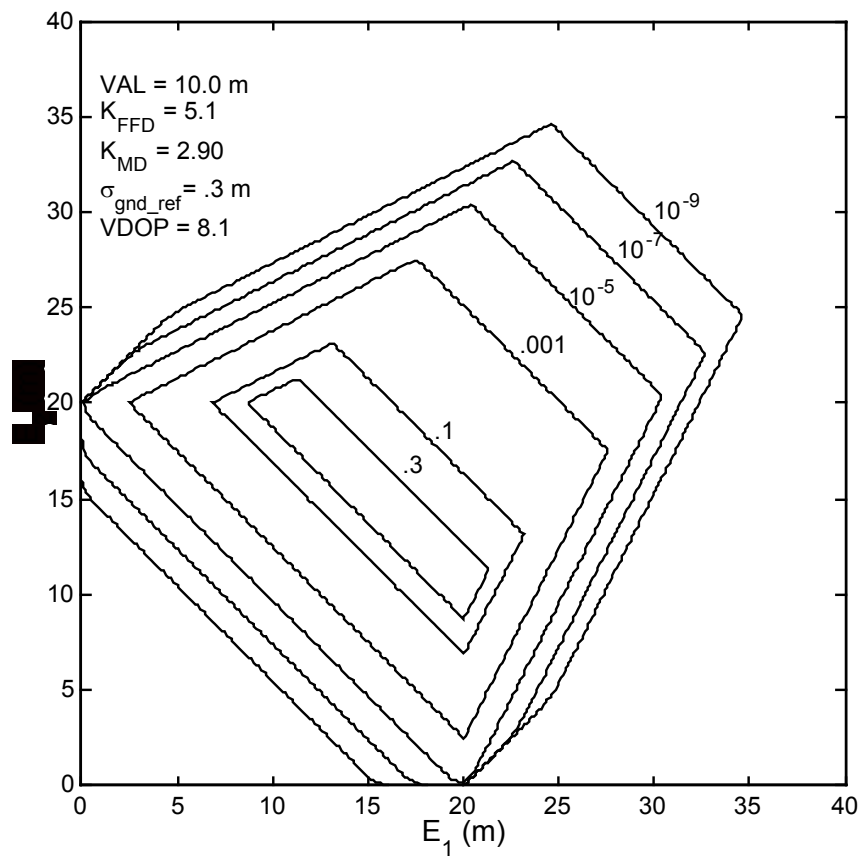
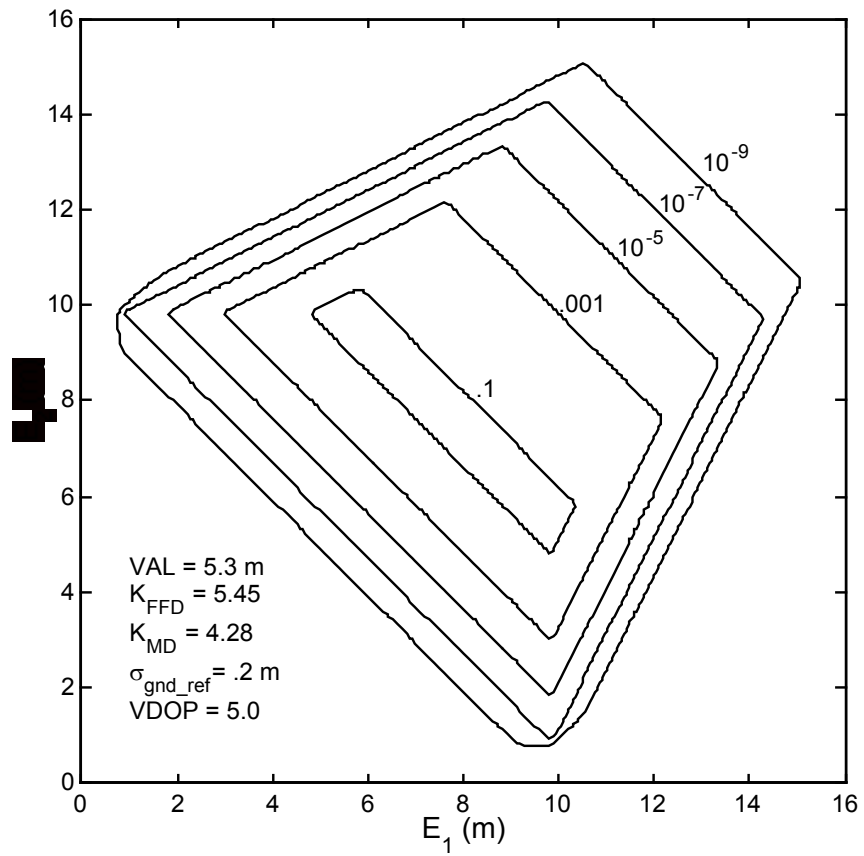


Figure 9. Conditional Probability of Misleading Information

Given E_1, E_2 for Worst Allowable Geometry (CAT I)



**Figure 10. Conditional Probability of Misleading Information
Given E_1, E_2 for Worst Allowable Geometry (CAT III)**

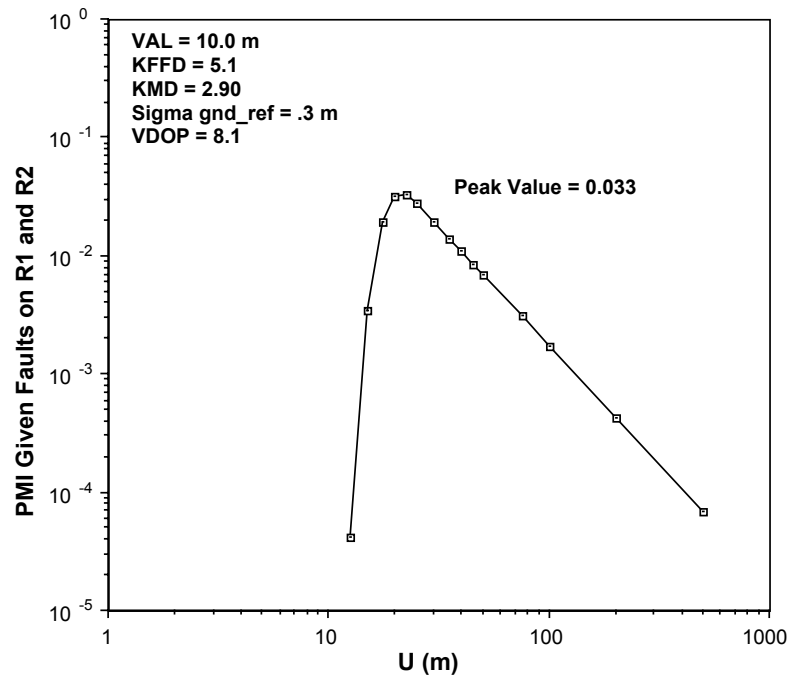


Figure 11. Probability of Misleading Information Assuming

E_1 and E_2 are Uniformly Distributed $[-U,U]$ (CAT I)

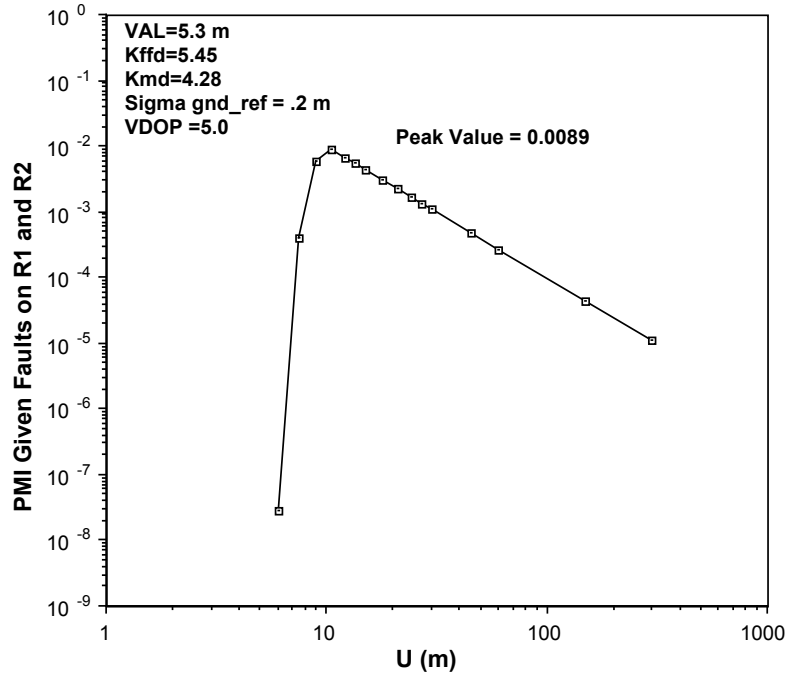


Figure 12. Probability of Misleading Information Assuming

E_1 and E_2 are Uniformly Distributed $[-U,U]$ (CAT III)